Veterinary Record Open

Cross-sectional area and fat content in dachshund epaxial muscles: an MRI and CT reliability study

Anna Fredrika Boström,[1] Anu K Lappalainen,[1] Lieven Danneels,[2] Tarja S Jokinen,[1] Outi Laitinen-Vapaavuori,[1] Anna K Hielm-Björkman[1]

► Additional material is published online only. To view please visit the journal online (http://dx.doi.org/10.1136/vetreco-2017-000256).

To cite: Boström AF, Lappalainen AK, Danneels L, *et al*. Cross-sectional area and fat content in dachshund epaxial muscles: an MRI and CT reliability study. *Veterinary Record Open* 2018;**5**:e000256. doi:10.1136/vetreco-2017-000256

Received 3 October 2017
Revised 7 February 2018
Accepted 13 February 2018

[1]Small Animal Surgery, Department of Equine and Small Animal Medicine, Faculty of Veterinary Medicine, University of Helsinki, Helsinki, Finland
[2]Department of Rehabilitation Sciences and Physiotherapy, Faculty of Medicine and Health Sciences, University of Ghent, Ghent, Belgium

Correspondence to
Dr Anna Fredrika Boström; anna.bostrom@helsinki.fi

ABSTRACT

MRI and CT are frequently used to diagnose spinal diseases in dogs. These modalities have detected epaxial muscle degeneration in dachshunds with intervertebral disc herniation. However, research on the reliability of epaxial muscular measurements is limited in veterinary medicine. The aims of the study were to assess the intrarater and inter-rater reliability of epaxial muscle cross-sectional area (CSA) and fat content measurements on MRI and CT images in dachshunds, and to compare the CSA measurement between the two modalities. MRI and CT images of 10 healthy dachshunds were evaluated. Two blinded observers assessed MRI CSA, MRI fat content, CT CSA and CT muscle attenuation of three thoracolumbar epaxial muscles using OsiriX. The results showed 'substantial' to 'almost perfect' intrarater reliability (intraclass correlation coefficient (ICC) 0.828–0.998) and inter-rater reliability (ICC 0.685–0.854) for all variables. When individual spinal segments were analysed, the intrarater and inter-rater reliability decreased and the confidence intervals increased. There was positive correlation (r= 0.719–0.841, P=0.001) and high agreement (0.824–0.894) for the measured CSA between MRI and CT. Epaxial muscle CSA and fat content can be reliably measured on MRI and CT, bearing in mind that measurement of certain segments requires adequate training.

INTRODUCTION

MRI and CT are frequently used in the diagnosis of canine intervertebral disc herniation (IVDH).[1 2] Previous MRI studies have detected changes in muscle structure, decreased cross-sectional area (CSA) and increased fat infiltration in theMusculi (Mm.) multifidi and Musculus (M.) longissimus dorsi muscles in dachshunds with IVDH compared with controls.[3 4] Also investigations using CT have found smaller paraspinal muscles in dogs with lumbosacral stenosis than in healthy dogs.[5 6] Similarly in human beings, back pain caused by IVDH has been shown to decrease CSA and increase fat infiltration of the paraspinal musculature.[7–9] These findings have helped clinicians to determine the clinical relevance of lesions, to predict recurrence of back pain, and to investigate effects of bed rest, surgery or different physiotherapy interventions.[7–13] Further investigation of the role of epaxial muscle atrophy in canine intervertebral disc disease would guide the planning of treatment and physiotherapeutic protocols to enhance recovery in dogs with back pain or after spinal surgery. Assessment of the spinal musculature in relation to disc changes would also help the veterinary surgeon to determine the clinical relevance of mild disc protrusions.

Atrophy (decreased CSA) and fat infiltration are two signs of muscle degeneration that can be evaluated with MRI and CT.[7–9] The CSA measured by MRI and CT is determined by the total quantity of muscle fibres and provides an objective measure of muscle size.[14] Fat infiltration may decrease the contractile ability of a muscle when muscle fibres are replaced by non-contractile fat tissue, resulting in altered muscle function.[9] Intramuscular fat is reliably quantified using the signal intensity obtained by MRI.[15] On MRI, the T1 relaxation time for fat tissue is short and the signal intensity is high compared with skeletal muscle on the T1-weighted (T1W) sequence. Therefore, fat appears hyperintense (lighter) relative to muscle, which is hypointense (darker).[9 15] Muscle density, another measure of muscle composition, can be estimated by the CT muscle attenuation value (Hounsfield units, HU).[16] Muscle density reflects the number of muscle fibres, the area of the individual muscle fibre and the contractile ability of each muscle fibre.[10] Fat displays attenuation values in the negative range and muscle tissue in the positive range relative to water. This means that fat tissue appears dark on the CT image and muscle brighter; a darker muscle with a lower attenuation value thus has a greater fat content.[17]

Although human paraspinal muscle atrophy and its relationship to spinal pathology have interested researchers for decades,[8 18 19] the

value of muscle atrophy as a marker of back pathology or as a predictor of back pain has been questioned.[20 21] Recent human studies stress the importance of using validated and well-reported muscular measurement methods to ensure reliable and comparable evaluation results of the images.[22 23] It is important to report factors related to objectivity and blinding of the research set-up, observer experience, as well as standardisation of scanning parameters and positioning of the patient.[22 24] Veterinary medicine lacks standardised, blinded and reliable methods to measure CSA and fat content from MRI and CT, and the inter-rater reliability of the evaluators also needs to be assessed.[3 5 6] Small animal hospitals and veterinary practices have CT and MRI available, but depending on the device, scanning positions may vary from lateral recumbency to dorsal or sternal recumbency. This introduces another difficulty for the development of standardised methods for muscle evaluation. Further research on epaxial muscle atrophy would benefit dogs recovering from back pain or spinal surgery. This study proposes a research method for future investigations on the relationship between epaxial muscles and spinal pathology to enhance the development of new treatment and rehabilitation strategies.

The aims of the study were to assess the intrarater and inter-rater reliability of epaxial muscle CSA and fat content measurement evaluated on MRI and CT images in clinically healthy dachshunds and to compare the CSA measurement between the two modalities. We hypothesised that the CSA and fat content of dachshund epaxial musculature would be reliably measured using both MRI and CT, but that the reliability would be higher using MRI.

MATERIALS AND METHODS

The study was undertaken at the Helsinki University Veterinary Teaching Hospital, Helsinki, Finland. T1W transverse MRI and transverse CT images from client-owned dachshunds considered healthy by their owners were investigated retrospectively. All dogs had participated in another study on the evaluation of intervertebral discs between MRI and CT. Inclusion criteria in our study were as follows: age 2–3.5 years, no history of back pain, no evidence of IVDH or spinal cord compression on either MRI or CT, and available transverse MRI and transverse CT images from the cranial aspect of the ninth thoracic vertebral body (T9) to the caudal aspect of the first lumbar vertebral body (L1). Exclusion criteria were lack of transverse slices and images from only MRI or CT. To account for possible influence of physical exercise on the muscular measurements, the dog's level of exercise regimen was quantified using an owner questionnaire. Written consent was obtained from dog owners.

Anaesthesia

The dogs were sedated intramuscularly in the M. biceps femoris according to individually adjusted dosages of dexmedetomidine hydrochloride (Orion-Pharma, Turku, Finland) and butorphanol (Richter Pharma, Wels, Austria). General anaesthesia was induced with intravenous injection of propofol (Zoetis Finland Oy, Helsinki, Finland) and maintained with inhaled isoflurane (Piramal Health Care, Northumberland, UK) and oxygen.

Imaging protocols

A low-field 0.24 T MRI scanner (Esaote SpA, Genoa, Italy) calibrated according to the hospital's daily procedure was used. The restricted space within the scanner entailed the dogs being positioned according to normal hospital practice, in right lateral recumbency. The same coil (9101819001 Esaote SpA) was used for all dogs. The T9–L1 area of the spine was scanned in the sagittal and transverse planes according to the following protocol: T1W spin echo sequences with time to echo 18 ms, time to repeat 830–970 ms, acquisition matrix 192×181, 4-mm slice thickness and interslice gap 10 per cent. MRI was performed first, followed immediately by CT.

CT images of the spine were obtained using a helical dual slice scanner (Siemens Somatom Emotion Duo, Siemens AG, Forchheim, Germany) with a soft tissue algorithm (B50). The CT scanner was calibrated daily according to the hospital's procedure. Scan parameters were as follows: 100 mA, 110 kV, 1.0-mm acquisition slice thickness, feed/rotation 2 mm, rotation time 0.8 s and reconstruction interval 0.5 mm. The dogs were positioned in dorsal recumbency according to normal hospital practice. The images were stored in Digital Imaging and Communications in Medicine format in the hospital's Picture Archiving and Communication System until analysis.

Measurement technique

To ensure measurements at the same transverse level in MRI and CT images, the following protocol was used: an European College of Veterinary Neurology (ECVN) Diplomate (TSJ) not involved in the muscular measurements performed the selection of the corresponding MRI and CT transverse images for every segment (T9–L1). First, a transverse MRI image was chosen based on visible nerve root canals at each intervertebral level. Thereafter, with help of additional landmarks and their shape, the corresponding transverse CT image was selected. The additional landmarks included articular facets, spinous processes, dorsal arches of the vertebrae, transverse processes, os costae and intervertebral discs (Fig 1a,b and Fig 2a,b).

The evaluation was done using digital imaging software (OsiriX V.6.5.2 Pixmeo, Bern, Switzerland). The MRI measurements were performed using full dynamic window (window level (WL) 1647, window width (WW) 3294, image size of 256×256). The measurements for the CT were made in the muscle window (WL 50, WW 400) and further adjusted in the bone window (WL 300, WW 1500) with an image size of 512×512.

FIG 1: Representative transverse T1-weighted MRI (a) and CT window level 300/window width 1500 (b) images at T9–10 in the same dog.

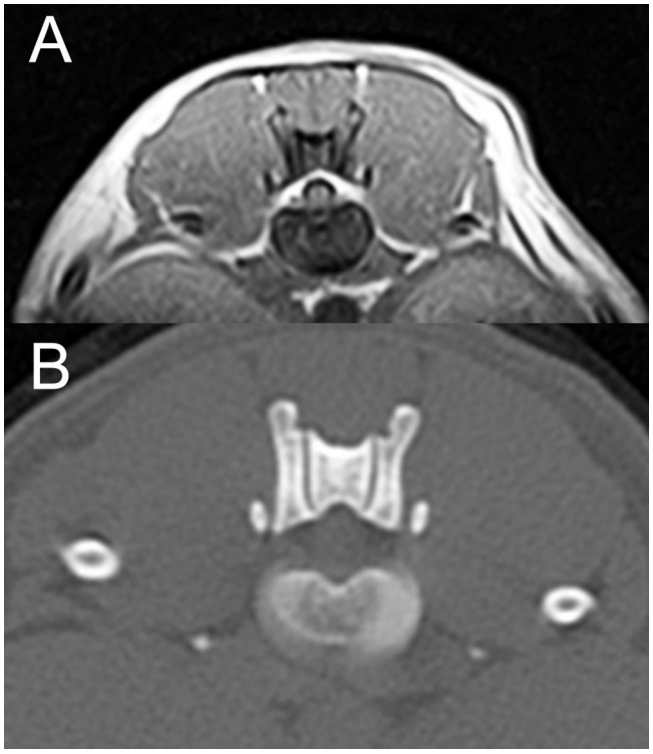

FIG 2: Corresponding transverse T1-weighted MRI (a) and CT window level 300/window width 1500 (b) images at T13–L1 in the same dog.

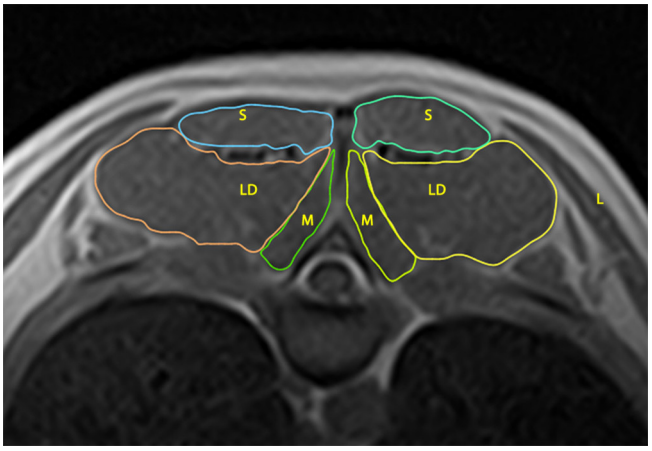

FIG 3: Transverse T1-weighted MRI at T9–10 showing the cross-sectional area for Mm. multifidi (M), M. spinalis et semispinalis (S) and M. longissimus (LD).

The muscle size (CSA cm^2) of the thoracolumbar Mm. multifidi, M. spinalis et semispinalis thoracis and Mm. longissimus thoracis et lumborum was measured bilaterally on both MRI and CT images (Figs 3 and 4). The M. spinalis et semispinalis muscle belly was not clearly visible caudally to T11 (Fig 5). Therefore this muscle was measured at only the first two segments (T9–T11). The CSA of each muscle was determined by manually drawing a region of interest (ROI) with the software's pencil tool, tracing the outer margin of each muscle. Possible intermuscular fat was excluded. When the boundary between the fat and muscle was unclear, the ROI was defined through the middle of this region to allow a reasonable approximation of the muscle's anticipated boundary.[25] The same routine was executed when the boundaries between M. longissimus and Mm. levatores costarum were indistinct. When the boundary between M. longissimus and M. iliocostalis was not evident, the M. iliocostalis was included in the M. longissimus measurement.

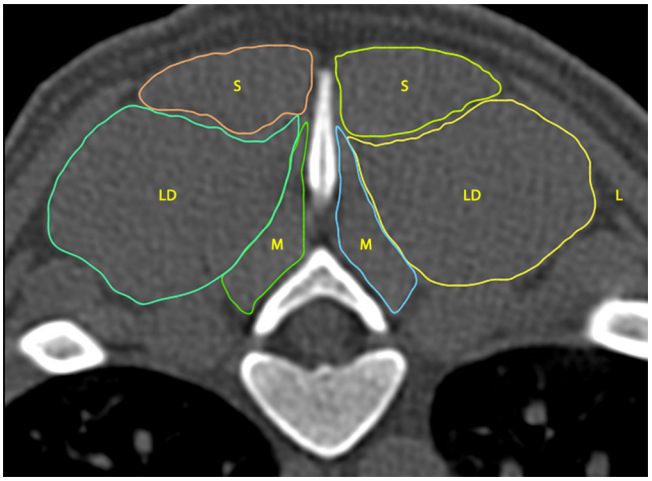

FIG 4: Transverse CT window level 300/window width 1500 image at T9–10 presents the cross-sectional area of Mm. multifidi (M), M. spinalis et semispinalis (S) and M. longissimus (LD).

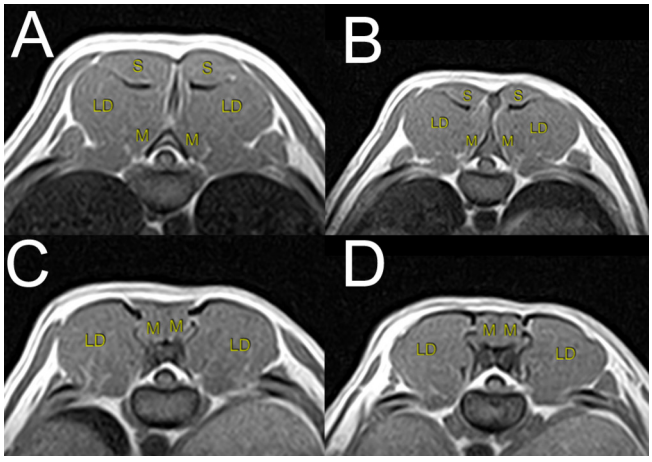

FIG 5: Transverse T1-weighted image series from T9–T13 showing the appearance of the Mm. multifidi (M), M. spinalis et semispinalis (S) and M. longissimus (LD) at each intervertebral segment (a) T9–10, (b) T10–11, (c) T11–12 and (d) T12–13.

The muscle fat content on MRI was calculated according to previous reports using the software-provided signal intensity from the muscle CSA ROI and from a small area of fat (Fig 6).[3 15] The study dogs were lean and fit, and therefore only a 5 mm^2 area of high signal intensity intermuscular fat was measurable. The fat ROI was drawn on the same image as the muscular measurements. Considering that signal intensity decreases with depth from the coil and to further ensure objectivity, the fat ROI was drawn in a standardised spot at the same depth as the midpoint of M. longissimus. The muscle fat content on CT was the software-provided muscle attenuation value (HU) obtained from individual muscle CSA ROIs (Fig 7).

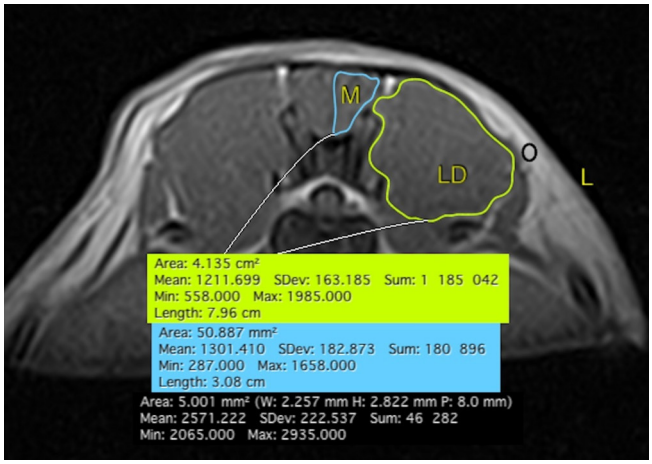

FIG 6: Transverse T1-weighted MRI at T13–L1 showing the calculation for the MRI fat content value for the left Mm. multifidi (M) and M. longissimus (LD). The MRI fat content value was calculated using the signal intensity mean of the muscle and the signal intensity mean of fat (black area) (ie, the MRI fat content value for the left side of the M. longissimus (LD); LD signal intensity mean, 1211.699/fat signal intensity mean, 2571.222).

A physiotherapist (AFB, observer 1) and a veterinary radiologist (AKL, observer 2) performed the measurements at five spinal levels (T9–10, T10–11, T11–12, T12–13 and T13–L1) in each of the 10 dogs, twice each, resulting in 200 sets of measured images. The MRI images were measured first, followed by the CT images. The images were mixed randomly between dogs and measurements were performed in a random order according to a computerised randomisation list. The observers were blinded to each other's evaluations and to the background data of the dogs. Review of measured images was not permitted. AFB had some experience with the investigated method from a previous study,[3] while AKL had no previous experience. AFB instructed AKL in the measurement technique and both practised independently until comfortable with the procedure.

Statistical analyses

The sample size of 10 dachshunds was estimated to be sufficient based on a power calculation using the M. multifidus and M. erector spinae fatty infiltrate variables from a human reliability study on paraspinal muscle volume and fat infiltration.[26] The data were assessed for normal distribution using the Kolmogorov-Smirnov and Shapiro-Wilk tests. Descriptive statistics were used to report the means and sd of age and bodyweight. The MRI and CT CSA, the MRI fat content value and CT muscle attenuation were investigated for each muscle bilaterally.

Intrarater reliability was investigated by comparing the measurements from the two occasions. The interrater reliability was investigated by comparing the measurements from all spinal segments on the first measurement occasion between the two observers. The agreement for the CSA was assessed between the two imaging modalities by comparing the measurements obtained from the first occasion. The intrarater agreements between the two measurement occasions and

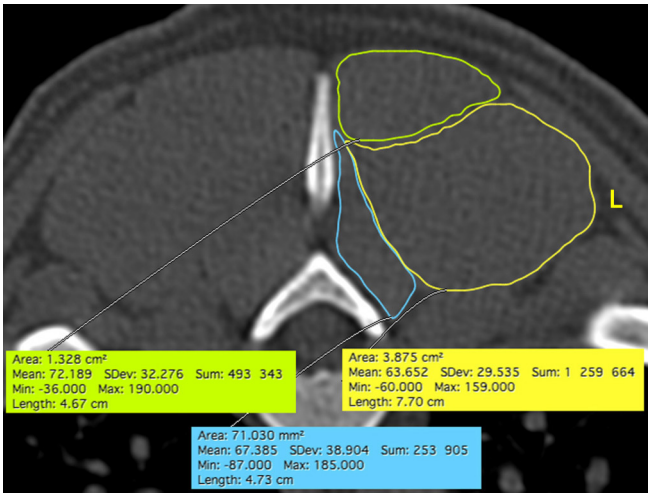

FIG 7: Transverse CT image from T9–10 showing the mean muscle attenuation value for the Mm. multifidi (67.385), M. spinalis et semispinalis (72.189) and M. longissimus (63.652) used in the analysis.

TABLE 1: Intrarater reliability: intraclass correlation coefficients and 95% confidence intervals for MRI and CT CSA variables for observers 1 and 2

	MRI CSA		CT CSA	
	Observer 1	Observer 2	Observer 1	Observer 2
Multifidus left, n=50	0.936 (0.837 to 0.970)	0.889 (0.699 to 0.949)	0.945 (0.903 to 0.969)	0.908 (0.805 to 0.953)
Multifidus right, n=50	0.909 (0.810 to 0.953)	0.898 (0.761 to 0.950)	0.926 (0.869 to 0.958)	0.852 (0.709 to 0.921)
Spinalis et semispinalis left, n=20	0.993 (0.983 to 0.997)	0.888 (0.144 to 0.970)	0.897 (0.741 to 0.959)	0.844 (0.602 to 0.938)
Spinalis et semispinalis right, n=20	0.984 (0.963 to 0.993)	0.874 (0.228 to 0.964)	0.967 (0.918 to 0.987)	0.929 (0.822 to 0.972)
Longissimus left, n=50	0.975 (0.956 to 0.986)	0.892 (0.649 to 0.954)	0.963 (0.935 to 0.979)	0.949 (0.910 to 0.971)
Longissimus right, n=50	0.977 (0.960 to 0.987)	0.907 (0.574 to 0.965)	0.985 (0.974 to 0.992)	0.952 (0.891 to 0.976)

CSA, cross-sectional area.

the inter-rater agreement between the two observers were analysed using a two-way mixed model and absolute agreement intraclass correlation coefficient (ICC), using 95 per cent confidence interval (CI). The analysis was performed both for the mean of all segments and for individual segments.

The CSA measurements between MRI and CT were compared using computed mean variables for the two observers to account for differences in observers' measurements. The agreement was tested with a two-way mixed model and absolute agreement ICC at 95 per cent CI and reported according to Landis and Koch,[27] thus 'slight agreement' 0.01–0.20, 'fair agreement' 0.21–0.40, 'moderate agreement' 0.41–0.60, 'substantial agreement' 0.61–0.80 and 'almost perfect' agreement 0.81–1.00. The correlation between the MRI and CT-acquired CSA mean variables was analysed with the two-tailed Pearson correlation test, for each muscle bilaterally.

Considering the different scanning positions in MRI (lateral recumbency) and CT (dorsal recumbency), we further tested whether there was a difference between left and right sides in the two scanning positions. The mean muscle variables between the left and right sides for individual segments were compared using the paired *t* test, and when data were not normally distributed, they were compared using the Wilcoxon signed-rank test. SPSS V.22 and V.24 were used in the analysis, and the level of significance was set at <0.05.

RESULTS

Ten dachshunds met the inclusion criteria for this study. They were all standard dachshunds, six entire males and four entire females. Their mean age was 2.7±sd 0.4 years and mean weight 9.6±sd 1.4 kg. All dogs had a moderate exercise level, defined as brisk walks for at least 20 minutes two to four times daily, where at least one of the walks lasted >1 hour. All dogs were allowed to run and play free regularly on a weekly basis and their exercise terrain consisted of several different surfaces.

Observer 1 demonstrated 'almost perfect' intrarater reliability for all measurements (ICC 0.828–0.993) (Tables 1 and 2). Observer 2 showed 'almost perfect' intrarater reliability for both MRI and CT measurements (ICC 0.844–0.998), except for the MRI fat value of the M. spinalis et semispinalis left, M. spinalis et semispinalis right and the M. longissimus left, for which the agreements were classified as 'substantial' (ICC 0.650–0.773) (Tables 1 and 2). When the analysis was limited to individual spinal segments, intrarater agreement for both observers decreased for the Mm. multifidi MRI CSA and MRI fat value (0.289–0.483) and for the M. spinalis et semispinalis MRI fat value (0.436) and CT CSA

TABLE 2: Intrarater reliability: intraclass correlation coefficients and 95% confidence intervals for MRI fat content and CT muscle attenuation variables for observers 1 and 2

	MRI fat content		CT muscle attenuation	
	Observer 1	Observer 2	Observer 1	Observer 2
Multifidus left, n=50	0.839 (0.716 to 0.909)	0.871 (0.676 to 0.896)	0.983 (0.970 to 0.990)	0.957 (0.925 to 0.977)
Multifidus right, n=50	0.952 (0.916 to 0.973)	0.939 (0.892 to 0.966)	0.946 (0.905 to 0.969)	0.967 (0.941 to 0.981)
Spinalis et semispinalis left, n=20	0.930 (0.833 to 0.971)	0.650 (0.225 to 0.841)	0.981 (0.952 to 0.992)	0.988 (0.970 to 0.995)
Spinalis et semispinalis right, n=20	0.926 (0.822 to 0.969)	0.773 (0.510 to 0.896)	0.964 (0.912 to 0.986)	0.947 (0.867 to 0.979)
Longissimus left, n=50	0.875 (0.780 to 0.929)	0.773 (0.602 to 0.871)	0.993 (0.988 to 0.996)	0.998 (0.978 to 0.993)
Longissimus right, n=50	0.828 (0.697 to 0.903)	0.872 (0.775 to 0.928)	0.993 (0.988 to 0.996)	0.996 (0.992 to 0.998)

TABLE 3: Inter-rater reliability: intraclass correlation coefficients with 95% confidence intervals between two observers for each muscular variable on the left and right sides

	MRI CSA	CT CSA	MRI fat content	CT muscle attenuation
Multifidus left, n=50	0.904 (0.831 to 0.946)	0.887 (0.801 to 0.936)	0.760 (0.577 to 0.863)	0.961 (0.931 to 0.978)
Multifidus right, n=50	0.880 (0.789 to 0.932)	0.890 (0.806 to 0.937)	0.851 (0.727 to 0.918)	0.970 (0.947 to 0.983)
Spinalis et semispinalis left, n=20	0.858 (0.653 to 0.942)	0.909 (0.744 to 0.966)	0.685 (0.200 to 0.877)	0.984 (0.961 to 0.994)
Spinalis et semispinalis right, n=20	0.866 (0.676 to 0.944)	0.948 (0.868 to 0.980)	0.762 (0.415 to 0.905)	0.959 (0.896 to 0.984)
Longissimus left, n=50	0.890 (0.591 to 0.959)	0.917 (0.437 to 0.972)	0.693 (0.378 to 0.839)	0.990 (0.981 to 0.994)
Longissimus right, n=50	0.871 (0.079 to 0.960)	0.909 (0.305 to 0.971)	0.854 (0.666 to 0.928)	0.987 (0.945 to 0.995)

CSA, cross-sectional area.

(0.055–0.495) at the T9–10 and T10–11 segments (online supplementary table 5).

There was 'almost perfect' inter-rater reliability between the two observers for the CSA measurements (ICC 0.866–0.948) (Table 3). The inter-rater reliability values for the MRI fat content varied between 'substantial' and 'almost perfect' for all muscles (0.685–0.854). The agreement for the CT muscle attenuation was 'almost perfect' for all measurements (0.959–0.987) (Table 3). Analysis of individual spinal segments showed 'moderate' inter-rater agreement for the Mm. multifidi MRI CSA and MRI fat value at the T10–11 segment (0.411–0.543) and 'slight' agreement for M. longissimus left MRI fat value at the T13–L1 segment (0.213) (online supplementary table 6).

The agreements between the MRI and CT for CSA were 'almost perfect' (0.824–0.894), and there was a high positive correlation (r=0.719–0.841) between MRI CSA and CT CSA with all P values <0.001 (Table 4).

No significant difference emerged in the CSA between the left and right sides on either MRI or CT other than the Mm. multifidi MRI-acquired CSA on the right side being significantly larger than the left side for the T11–12 spinal segment (P=0.028). The Mm. multifidi MRI fat content on the right side was significantly higher at the T10–11 segment than on the left side (P=0.005). The MRI fat content for the longissimus muscle on the right side was significantly higher for all segments relative to the left side: T9–10 (P=0.009), T10–11 (P=0.005), T11–12 (P=0.005), T12–13 (P=0.005) and T13–L1 (P=0.007). The CT muscle attenuation for Mm. multifidi was higher on the left (P=0.017) and the CT muscle attenuation for M. spinalis et semispinalis was higher on the right at the T10–11 segment (P=0.047).

TABLE 4: Correlation and agreement between MRI and CT for cross-sectional area (CSA) with the intraclass correlation coefficient (ICC), the Pearson correlation coefficient (r) and significant P values

	CSA correlation		CSA ICC
	r	P value	ICC (95% CI)
Multifidus left, n=50	0.784	<0.001	0.860 (0.726 to 0.925)
Multifidus right, n=50	0.719	<0.001	0.826 (0.593 to 0.901)
Semispinalis left, n=20	0.772	<0.001	0.866 (0.650 to 0.948)
Semispinalis right, n=20	0.805	<0.001	0.894 (0.731 to 0.958)
Longissimus left, n=50	0.794	<0.001	0.824 (0.411 to 0.927)
Longissimus right, n=50	0.841	<0.001	0.889 (0.734 to 0.946)

DISCUSSION

The results of this study suggest that the muscle structure in terms of CSA and fat content of the thoracolumbar epaxial muscles in healthy dachshunds can be reliably and repeatedly measured from both MRI and CT. In the analysis of individual segments, there was large variation in the CIs for several variables, particularly for MRI fat content and MRI CSA. This indicates that the T9–10 and T10–11 segments were difficult to measure in a consistent way; however, good correlation existed for the CSA measurement between MRI and CT.

The intrarater reliability of the two observers was in accordance with canine and human high-field MRI studies that showed good to excellent intrarater reliability (ICC 0.870–0.990).[3 7 15] Observer 2 had somewhat wider variation than observer 1 in the 95 per cent CIs for MRI CSA. Difference in experience is a likely explanation for this finding. The more experienced observer usually has higher intrarater reliability and smaller muscles require greater experience to produce accurate measures.[22] Both observers were considered novices relative to human studies, where observer experience of several years has been reported.[20] Nevertheless, despite their different specialist training and experience, it is possible to achieve acceptable results even with only moderate experience as long as adequate training takes place.[3 22]

The inter-rater reliability was excellent for several variables on MRI and CT. This high inter-rater reliability is in line with previous studies that found good to excellent inter-rater reliability in drawing ROIs in human neck muscles.[15 28] However, there was a large variation in the 95 per cent CIs in the MRI CSA for M. longissimus and in the MRI fat content for Mm. multifidi left, M. spinalis et semispinalis left and right, and M. longissimus left. There may be several reasons for this, such as observers' training and experience

discussed above and poor resolution of low-field MRI. The decreased level of agreement for the Mm. multifidi when the analysis was restricted to individual segments indicates that particularly the T9–10 and T10–11 segments were difficult to measure. At these segments, vertebral bony structures were not as evident and the resolution in low-field MRI images was insufficient to distinguish the Mm. multifidi and M. longissimus muscle borders accurately. Furthermore, due to partial volume effect, the higher slice thickness of MRI images may have had an effect on the accuracy of measurements of smaller structures especially. One human MRI study suggests that if a repeatable measurement of lesion size is required, then the slice thickness should be at most one-fifth of the lesion size.[29] Further research on muscular measurements in small animals and on certain segments should consider the use of high-field MRI because of the superior resolution. The variance in the CIs highlights the importance of assessing also inter-rater reliability and reporting the CIs when a novel method is investigated. Additionally, we used T1W MRI to evaluate the fat infiltration of the muscles. Our approach was to compare the signal intensity from the muscle CSA ROI and from a small area of subcutaneous fat. This approach has been used in human studies,[30 31] but may be problematic in lean animals, or when signal quality of a chosen area of subcutaneous fat is poor. To over-ride this problem, future research may utilise a 2-point Dixon fat/water separation MRI technique for quantification of intramuscular adipose tissue.[32]

There was consistent intrarater and inter-rater agreement for CT CSA and CT muscle attenuation. A risk for overestimation of linear measurements on CT has previously been proposed.[33] To account for possible overestimation and to reduce bony artefacts, we drew the ROIs first in the muscle window to provide a clear view of the muscle borders and then adjusted the ROI to the bony landmarks in the bone window. This procedure may have brought additional precision to the CT measurements in comparison with the MRI, hence the larger consistency in the CT measurements.

Still, the results indicate that the measured CSAs of the investigated thoracolumbar muscles are comparable between MRI and CT. The high agreement between observers for the CT variables and the consistent 95 per cent CIs relative to the MRI variables suggest that CT would be the more reliable imaging modality in the dachshunds studied. However, it should be kept in mind that there are differences between the intrinsic characters of the modalities. Drawing ROIs on CT images is more approximate than drawing on MRI images because CT has a poorer soft tissue resolution than MRI. However, on low-field MRI images, the spatial resolution may be insufficient relative to the small structures measured, hence the greater variance in the CIs and the decrease in reliability. Furthermore, due to partial volume effect, the smaller slice thickness in CT compared with MRI may have had an influence on the CSA measurements, thus giving higher agreement in the measured CSA from CT images. By contrast, a human study on paraspinal muscle size and fat infiltration showed higher intrarater (0.910) and inter-rater reliability (0.890) for MRI than for CT (intrarater reliability 0.780, inter-rater reliability 0.650).[14] Not surprisingly the CSA is more reliably measured by MRI than by CT in human subjects because human muscles are larger and high-field scanners (1.5–3.0 T) are generally used.[14 22]

No significant difference was present in the CSAs between the left and right sides on either MRI or CT, suggesting that the scanning position did not influence the CSA measurement. However, the MRI fat content for the M. longissimus was significantly higher on the right side in all segments. Positioning the dogs in lateral recumbency may have resulted in asymmetrical loading of the coil, altering the relative signal intensity. This could have resulted in signal intensity artefacts,[34] possibly affecting the MRI fat content measurement. The inconsistent differences between sides for the CT muscle attenuation at the T10–11 segment can be explained by the variations in vertebrae anatomy and the previously mentioned difficulty in drawing the ROIs at this segment.

In human beings, the CSA, muscular fat content and CT attenuation may differ between patients due to variety in exercise levels, and furthermore differences may exist between individual muscles, different spinal segments and between left and right sides.[11 16 20 35] We report therefore the reliability with CIs in dachshunds of similar age, weight and exercise level, for each individual muscle on both the left and right sides at every measured segment in the thoracolumbar area T9–L1. By having such a homogeneous group, we avoided many confounding factors that have been discussed to affect the interpretation of results in previous studies.[22 24]

This study has some limitations. The inclusion of only healthy subjects may have caused a selection bias, making the methodology appear more reliable than if measuring atrophied muscles of actual patients with IVDH. Due to prolonged anaesthesia, it was not possible to obtain transverse slices from the whole range of spinal segments frequently affected with IVDH (T10–L3). However, the measured range covered the thoracolumbar area with most anatomical variations in the musculature.[36] The restriction of the analysis to individual segments caused a decrease in sample size, introducing another limitation when interpreting the results.

CONCLUSIONS

We conclude that muscle structure, measured as CSA and fat content, in dachshunds can be reliably evaluated using either MRI or CT. However, training is recommended to decrease the variations in the CIs

since evaluation of small muscles in specific spinal regions may show a lower degree of reliability. Testing all new observers' repeatability should ensure reliability in future studies. CSA measurement is comparable between MRI and CT, but researchers should favour imaging in identical scanning positions. Further studies could investigate the potential of this method to detect muscle changes in mild disc protrusions or in relation to physical training programmes.

Acknowledgements The authors thank Alana Rosenblatt, DVM, for her assistance with data collection, and Raimonda Uosyte, DVM, and Mindaugas Rakauskas, DVM, for their assistance with interpretation of the results.

Contributors AFB designed the study, collected and analysed the data, and drafted and revised the manuscript. AKL designed the study, collected the data and revised the manuscript. LD designed the study, interpreted the results and revised the manuscript. TSJ collected the data and revised the manuscript. OL-V designed the study, interpreted the results and revised the manuscript. AKH-B designed the study, analysed the data and revised the manuscript. All authors have approved the final version to be published.

Funding This work was supported in part by the Finnish Veterinary Foundation.

Competing interests None declared.

Patient consent Not required.

Ethics approval The National Animal Experiment Board (ESAVI/5794/04.10.03/2011) approved the study protocol.

Provenance and peer review Not commissioned; externally peer reviewed.

Data sharing statement All data available are published in this article or provided as online supplementary materials. Unpublished data are not available.

REFERENCES

1. Cooper JJ, Young BD, Griffin JF, *et al*. Comparison between noncontrast computed tomography and magnetic resonance imaging for detection and characterization of thoracolumbar myelopathy caused by intervertebral disk herniation in dogs. *Vet Radiol Ultrasound* 2014;55:182–9.
2. Moore SA, Early PJ, Hettlich BF. Practice patterns in the management of acute intervertebral disc herniation in dogs. *J Small Anim Pract* 2016;57:409–15.
3. Boström AF, Hielm-Björkman AK, Chang YM, *et al*. Comparison of cross sectional area and fat infiltration of the epaxial muscles in dogs with and without spinal cord compression. *Res Vet Sci* 2014;97:646–51.
4. Lerer A, Nykamp SG, Harriss AB, *et al*. MRI-based relationships between spine pathology, intervertebral disc degeneration, and muscle fatty infiltration in chondrodystrophic and non-chondrodystrophic dogs. *Spine J* 2015;15:2433–9.
5. Henderson AL, Hecht S, Millis DL. Lumbar paraspinal muscle transverse area and symmetry in dogs with and without degenerative lumbosacral stenosis. *J Small Anim Pract* 2015;56:618–22.
6. Cain B, Jones JC, Holásková I, *et al*. Feasibility for measuring transverse area ratios and asymmetry of lumbosacral region paraspinal muscles in working dogs using computed tomography. *Front Vet Sci* 2016;3.
7. Battié MC, Niemelainen R, Gibbons LE, *et al*. Is level- and side-specific multifidus asymmetry a marker for lumbar disc pathology? *Spine J* 2012;12:932–9.
8. Danneels LA, Vanderstraeten GG, Cambier DC, *et al*. CT imaging of trunk muscles in chronic low back pain patients and healthy control subjects. *Eur Spine J* 2000;9:266–72.
9. D'hooge R, Cagnie B, Crombez G, *et al*. Increased intramuscular fatty infiltration without differences in lumbar muscle cross-sectional area during remission of unilateral recurrent low back pain. *Man Ther* 2012;17:584–8.
10. Kalichman L, Hodges P, Li L, *et al*. Changes in paraspinal muscles and their association with low back pain and spinal degeneration: CT study. *Eur Spine J* 2010;19:1136–44.
11. Bouche KG, Vanovermeire O, Stevens VK, *et al*. Computed tomographic analysis of the quality of trunk muscles in asymptomatic and symptomatic lumbar discectomy patients. *BMC Musculoskelet Disord* 2011;12:1471–2474.
12. Hides JA, Lambrecht G, Richardson CA, *et al*. The effects of rehabilitation on the muscles of the trunk following prolonged bed rest. *Eur Spine J* 2011;20:808–18.
13. Gildea JE, Hides JA, Hodges PW. Size and symmetry of trunk muscles in ballet dancers with and without low back pain. *J Orthop Sports Phys Ther* 2013;43:525–33.
14. Hyun SJ, Bae CW, Lee SH, *et al*. Fatty degeneration of the paraspinal muscle in patients with degenerative lumbar kyphosis: a new evaluation method of quantitative digital analysis using MRI and CT scan. *Clin Spine Surg* 2016;29:441–7.
15. Elliott JM, Galloway GJ, Jull GA, *et al*. Magnetic resonance imaging analysis of the upper cervical spine extensor musculature in an asymptomatic cohort: an index of fat within muscle. *Clin Radiol* 2005;60:355–63.
16. Anderson DE, D'Agostino JM, Bruno AG, *et al*. Variations of CT-based trunk muscle attenuation by age, sex, and specific muscle. *J Gerontol A Biol Sci Med Sci* 2013;68:317–23.
17. Goodpaster BH, Thaete FL, Kelley DE. Composition of skeletal muscle evaluated with computed tomography. *Ann N Y Acad Sci* 2000;904:18–24.
18. Hides JA, Stokes MJ, Saide M, *et al*. Evidence of lumbar multifidus muscle wasting ipsilateral to symptoms in patients with acute/subacute low back pain. *Spine* 1994;19:165–72.
19. MacDonald DA, Moseley GL, Hodges PW. The lumbar multifidus: does the evidence support clinical beliefs? *Man Ther* 2006;11:254–63.
20. Niemeläinen R, Briand MM, Battié MC. Substantial asymmetry in paraspinal muscle cross-sectional area in healthy adults questions its value as a marker of low back pain and pathology. *Spine* 2011;36:2152–7.
21. Suri P, Fry AL, Gellhorn AC. Do muscle characteristics on lumbar spine magnetic resonance imaging or computed tomography predict future low back pain, physical function, or performance? A systematic review. *Pm R* 2015;7:1269–81.
22. Valentin S, Yeates TD, Licka T, *et al*. Inter-rater reliability of trunk muscle morphometric analysis. *J Back Musculoskelet Rehabil* 2015;28:181–90.
23. Crawford RJ, Cornwall J, Abbott R, *et al*. Manually defining regions of interest when quantifying paravertebral muscles fatty infiltration from axial magnetic resonance imaging: a proposed method for the lumbar spine with anatomical cross-reference. *BMC Musculoskelet Disord* 2017;18:25.
24. Keller A, Gunderson R, Reikerås O, *et al*. Reliability of computed tomography measurements of paraspinal muscle cross-sectional area and density in patients with chronic low back pain. *Spine* 2003;28:1455–60.
25. Fortin M, Battié MC. Quantitative paraspinal muscle measurements: inter-software reliability and agreement using OsiriX and ImageJ. *Phys Ther* 2012;92:853–64.
26. Valentin S, Licka T, Elliott J. Age and side-related morphometric MRI evaluation of trunk muscles in people without back pain. *Man Ther* 2015;20:90–5.
27. Landis JR, Koch GG. The measurement of observer agreement for categorical data. *Biometrics* 1977;33:159–74.
28. Elliott J, Jull G, Noteboom JT, *et al*. Fatty Infiltration in the Cervical Extensor Muscles in Persistent Whiplash-Associated Disorders. *Spine* 2006;31:E847–55.
29. Firbank MJ, Coulthard A, Harrison RM, *et al*. Partial volume effects in MRI studies of multiple sclerosis. *Magn Reson Imaging* 1999;17:593–601.
30. Elliott J, Sterling M, Noteboom JT, *et al*. Fatty infiltrate in the cervical extensor muscles is not a feature of chronic, insidious-onset neck pain. *Clin Radiol* 2008;63:681–7.
31. Elliott J, Pedler A, Kenardy J, *et al*. The temporal development of fatty infiltrates in the neck muscles following whiplash injury: an association with pain and posttraumatic stress. *PLoS One* 2011;6:e21194.

32. Smith AC, Parrish TB, Abbott R, *et al*. Muscle-fat MRI: 1.5 Tesla and 3.0 Tesla versus histology. *Muscle Nerve* 2014;50:170–6.
33. De Decker S, Gielen IM, Duchateau L, *et al*. Agreement and repeatability of linear vertebral body and canal measurements using computed tomography (CT) and low field magnetic resonance imaging (MRI). *Vet Surg* 2010;39:28–34.
34. Jones RW, Witte RJ. Signal intensity artifacts in clinical MR imaging. *Radiographics* 2000;20:893–901.
35. Hu ZJ, He J, Zhao FD, *et al*. An assessment of the intra- and inter-reliability of the lumbar paraspinal muscle parameters using CT scan and magnetic resonance imaging. *Spine* 2011;36:E868–E874.
36. Evans H. *Miller's Anatomy of The Dog*. 3rd edn. Pennsylvania: Saunders, 1993:290–302.